Rotating Ring-Disk Electrodes

III. Catalytic and ECE Reactions

Keith B. Prater[1] and Allen J. Bard*

Department of Chemistry, The University of Texas at Austin, Austin, Texas 78712

ABSTRACT

Digital simulation techniques were employed to calculate the ring and disk currents at the rotating ring-disk electrode (RRDE) for the cases where the intermediate generated at the disk electrodes undergoes first- or second-order processes producing electroactive species: either the original starting material (a catalytic reaction) or a new species (an ECE reaction). Working curves which allow the detection of these mechanisms and the determination of rate constants of the homogeneous reactions from current-rotation rate data are provided. The determination of the rate constant of the iron(II)-hydrogen peroxide reaction by examination of the reduction of iron(III) in a hydrochloric acid medium at a carbon paste RRDE is described.

A digital simulation treatment of the rotating ring-disk electrode (RRDE) in the absence of following chemical reactions has been presented previously (1). The results of this treatment were in excellent agreement with the work of Albery and Bruckenstein (2). This digital simulation technique has also been applied to those cases in which a following first- or second-order chemical reaction results in a nonelectroactive product (an EC mechanism) (3). These results were in good agreement with the approximate treatments of Albery and Bruckenstein (4-7) within the range of their approximations. In this paper, results of the digital simulation of two mechanisms in which the products of the following chemical reaction are electroactive at the potential of the disk electrode are presented.

In the first mechanism, the ECE (electrochemical-chemical-electrochemical) mechanism, species B, which is generated at the disk electrode by

$$A \pm n_1 e \rightarrow B \qquad [1]$$

undergoes a homogeneous reaction to yield species D which immediately undergoes a further electrochemical reaction at the disk electrode. The homogeneous reaction may be either first- or second-order. In the first-order case

$$B \xrightarrow{k_1} D \qquad [2]$$

while in the second-order case

$$B + C \xrightarrow{k_2} D + Y \qquad [3]$$

In either case, species D is immediately oxidized or reduced at the disk by

$$D \pm n_2 e \rightarrow Z \qquad [4]$$

and species C, Y, and Z are considered to be nonelectroactive at the potentials of the ring and disk electrodes. At the ring electrode, A is regenerated from B by the reaction

$$B \pm ne \rightarrow A \qquad [5]$$

The second mechanism is the so-called catalytic mechanism in which one of the products of the homogeneous reaction is the initial species, A. In the common second-order catalytic mechanism, the intermediate, B, reacts with species C, to yield A and Y, where C and Y are nonelectroactive. That is

$$B + C \xrightarrow{k_2} A + Y \qquad [6]$$

In the limit of large concentrations of species C, the second-order catalytic case simplifies to the first-order case given by

$$B \xrightarrow{k_1} A \qquad [7]$$

In each case, the chemical reaction is instantaneously followed by the re-oxidation or re-reduction of A to B as shown in Eq. [1]. As before, the reaction at the ring electrode is given by Eq. [5].

Digital Simulation

The ECE mechanism.—The general approach to the simulations and the notation to be used has been described in previous communications (1, 3). In the ECE mechanism, the ring current-dependent parameter, ZR, calculated for a given value of the rate parameter XKT for a first-order reaction or $XKTC$ for a second-order reaction, is identical with that calculated for the analogous EC case (3). The difference in the collection efficiency curves for the EC and ECE mechanisms is a result of the effect of the ECE reaction on the disk current parameter, ZD. Although the EC reaction does not change the disk current from that observed in the absence of a following reaction, the ECE reaction gives rise to increased disk current. Thus the collection efficiency working curves for the first- and second-order ECE mechanisms can be generated by calculating the ECE disk current for a specified value of the rate parameter and dividing the analogous EC ring current by that disk current.

The simulation of the first- and second-order ECE disk currents is quite similar to the previous RRDE simulation (1, 3) except that only the $K = 1$ boxes need to be considered and thus radial convection can be ignored. The dimensionless rate parameters, XKT and $XKTC$, are identical to those for the EC cases. The only major differences between the EC and ECE calculations are that in the ECE case, the boundary conditions at the disk electrode and the current parameter, ZD, must take into account the fact that both species A and species D are being consumed at the disk and that both are contributing to the total disk current. Thus in this case the parameter, ZD, will be the sum of the currents due to (i) diffusion of A into the disk box ($J = 1$, $K = 1$), (ii) diffusion of D into the disk box, and (iii) electrolysis of any D generated in the disk box. Since the fractional concentrations of A and D in the disk box are zero, the

* Electrochemical Society Active Member.
[1] Present address: University of Texas at El Paso, El Paso, Texas 79999.
Key words: digital simulation, electrode reactions, rotating disk electrode.

contribution to the current due to diffusion of A and D into the disk box will be

$$IA = DM_A F_A(2,1)\,(L/DM_A)^{1/2} \quad [8]$$

$$ID_{dif} = DM_D F_D(2,1)\,(L/DM_A)^{1/2} \quad [9]$$

The contribution to ZD due to electrolysis of D produced in the disk box will be

$$ID_{elec} = F_D(1,1)\,(L/DM_A)^{1/2}/2 \quad [10]$$

The factor of 1/2 occurs because the disk box is only $x/2$ wide. Thus in this case

$$ZD = IA + ID_{dif} + ID_{elec} \quad [11]$$

The simulated limiting disk currents as functions of the appropriate dimensionless rate parameters for the first- and second-order ECE mechanisms are shown in Fig. 1. The first-order curve agrees with that simulated by Feldberg *et al.* (8). The disk currents have been normalized by the disk current one would observe in the absence of any following reactions. These disk currents were calculated assuming the stoichiometry given in Eq. [3] and assuming that the number of electrons transferred per molecule is the same for the A to B reaction and the D to Z reaction. In those cases where $n_1 \neq n_2$ or where the stoichiometry is not 1 to 1, the disk current curves can easily be generated by multiplying the amount by which the disk current is enhanced by the appropriate factor. Also shown in Fig. 1 are the associated ring currents from the EC calculations for an electrode with $IR1 = 83$, $IR2 = 94$, and $IR3 = 159$. These, too, have been normalized by the ring current in the absence of any following reaction. The collection efficiency working curves for the first- and second-order ECE mechanisms are shown in Fig. 2. As must be the case, the collection efficiency is lower for an ECE curve than for the analogous EC curve.

The catalytic mechanism.—In the case of the catalytic mechanism, the ring current parameters, ZR, are not the same as the corresponding parameters in the EC mechanism, because the homogeneous reaction regenerating A at the disk is followed by reduction of A to B, so that a greater flux of B to the ring electrode is observed. The simulation, however, is entirely analogous to the simulation of the EC and ECE cases except for the appropriate changes in the boundary conditions and current parameters.

The simulated limiting disk currents for the catalytic mechanism as compared with those in the absence of a following reaction are shown in Fig. 3 as functions of XKT and $XKTC$. The limiting disk currents for this

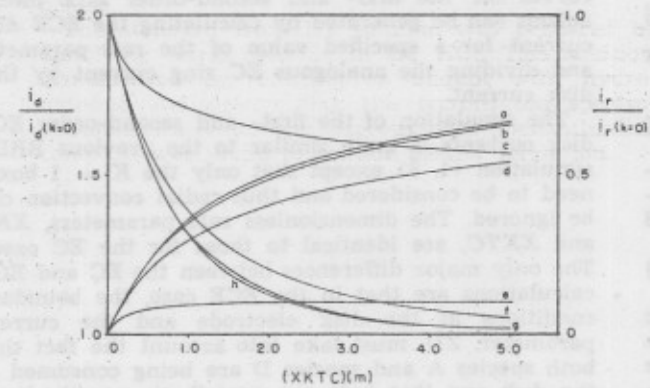

Fig. 1. Simulated limiting ring and disk currents for the ECE mechanism for various values of $m = C^\circ_C/C^\circ_A$. a. Disk current: first-order; b. disk current: $m = 10.0$; c. ring current: $m = 0.1$; d. disk current: $m = 1.0$; e. disk current: $m = 0.1$; f. ring current: $m = 1.0$; g. ring current: $m = 10.0$; h. ring current: first-order. $IR1 = 83$, $IR2 = 94$, $IR3 = 159$. $XKTC = k_2 C^\circ_A \omega^{-1} \nu^{1/3} D^{-1/3} (0.51)^{-2/3}$.

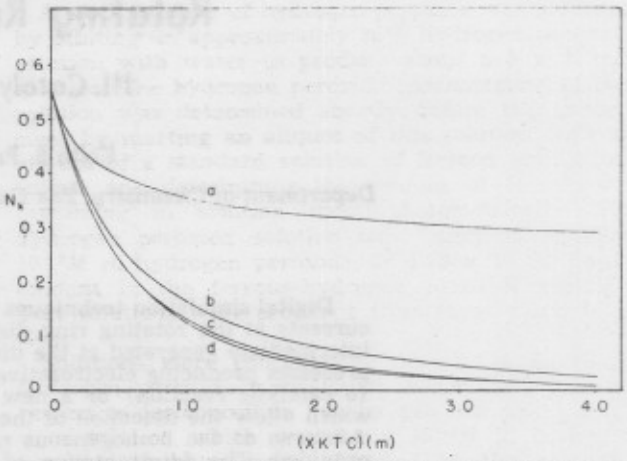

Fig. 2. Simulated collection efficiency vs. $(XKTC)$ (m) for the ECE mechanism for various values of m. a. 0.1; b. 1.0; c. 10.0; d. first-order. $IR1 = 83$, $IR2 = 94$, $IR3 = 159$. $XKTC = k_2 C^\circ_A \omega^{-1} \nu^{1/3} D^{-1/3} (0.51)^{-2/3}$. $m = C^\circ_C/C^\circ_A$.

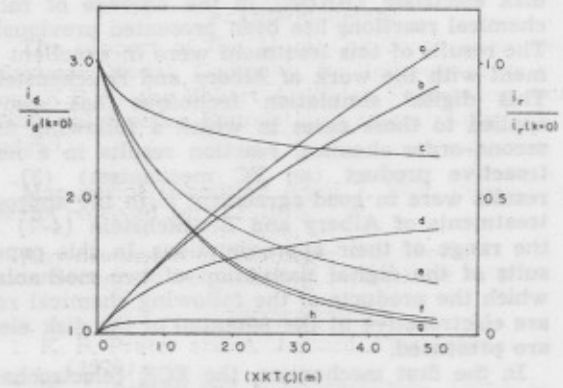

Fig. 3. Simulated limiting ring and disk currents for the catalytic mechanism for various values of m. a. Disk current: first-order; b. disk current: $m = 10.0$; c. ring current: $m = 0.1$; d. disk current: $m = 1.0$; e. ring current: $m = 1.0$; f. ring current: $m = 10.0$; g. ring current: first order; h. disk current: $m = 0.1$. $IR1 = 83$, $IR2 = 94$, $IR3 = 159$. $XKTC = k_2 C^\circ_A \omega^{-1} \nu^{1/3} D^{-1/3} (0.51)^{-2/3}$. $m = C^\circ_C/C^\circ_A$.

case have been treated by Koutecky and Levich (9), by Haberland and Landsberg (10), and by Beran and Bruckenstein (11). The treatment by Koutecky and Levich assumed that the reaction layer thickness was very small compared with the diffusion layer thickness, that is, it assumed that k/ω was large. Beran and Bruckenstein treated a rather complex system under pseudo-first order conditions. The simulation results agree very well with the more general treatment of Haberland and Landsberg. This is shown in Fig. 4 in which some of their data for the Fe^{+3}/H_2O_2 system are compared with points calculated from their data in the absence of the following reaction, the rate constant which they calculated, and the simulation results.

While the simulated disk currents are valid for any geometry, the limiting ring currents which are also shown in Fig. 3 were calculated for an electrode with $IR1 = 83$, $IR2 = 94$, and $IR3 = 159$. From the ring and disk currents, one can obtain the collection efficiency working curves shown in Fig. 5.

At this point it is appropriate to compare the simulated collection efficiency working curves for the EC, ECE, and catalytic mechanisms. In all useful ranges of the rate parameters, the ECE curves differ significantly from the analogous EC and catalytic curves. The collection efficiency found for the ECE mechanism for a given value of $XKTC$ and m, where $m = C^\circ_C/C^\circ_A$, is always smaller than that found for the

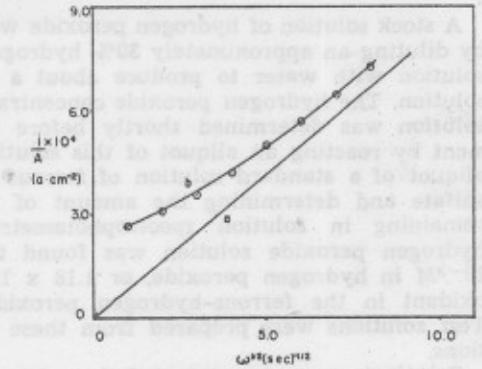

Fig. 4. Comparison of simulated disk current for the catalytic mechanism with results of Haberland and Landsberg (10) for the Fe^{+3}/H_2O_2 system. a. Limiting disk current in the absence of H_2O_2; b. simulated limiting disk current based on curve a, the homogeneous rate constant (k_2 = 145 liters/mole sec) calculated by Haberland and Landsberg and for $C_{H_2O_2} = 10\ C_{Fe^{+3}}$. ⊙ Experimental limiting currents found by Haberland and Landsberg for $C_{H_2O_2} = 1.6 \times 10^{-2}M$, and $C_{Fe^{+3}} = 1 \times 10^{-3}M$ in 1M KCl.

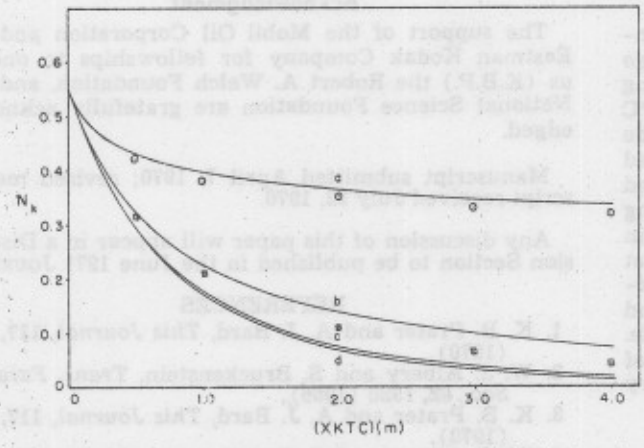

Fig. 5. Simulated collection efficiency *vs.* *XKTC(m)* for the catalytic mechanism for various values of m. a. 0.1; b. 1.0; c. 10.0; d. first-order. *IR1* = 83, *IR2* = 94, *IR3* = 159. $XKTC = k_2 C^\circ_A \omega^{-1} \nu^{1/3} D^{-1/3} (0.51)^{-2/3}$. $m = C^\circ_C / C^\circ_A$. ⊙ Simulated collection efficiency for the EC mechanism, $m = 0.1$. ⊡ Simulated collection efficiency for the EC mechanism, $m = 1.0$.

EC or catalytic mechanisms with the same values of *XKTC* and *m*. On the other hand, the EC and catalytic curves are, for most values of the rate parameters, quite similar. In fact, the first-order curves for the two mechanisms are indistinguishable as are the analogous curves for $m = 10.0$. The $m = 1.0$ and $m = 0.1$ curves for the two mechanisms are experimentally indistinguishable for values of $(XKTC \cdot m) < 0.5$. Thus, it is not surprising that Albery *et al.* (6) obtained reasonable results when they treated a pseudo-first order catalytic system with a theory developed for the EC mechanism. Although the collection efficiency data are insufficient for differentiating between the EC and catalytic mechanism, examination of the limiting ring and disk currents allows the two mechanisms to be easily distinguished. The limiting disk current for the EC mechanism is identical to that found in the absence of any following reaction, while the limiting disk current, i_{lim}, for the catalytic mechanism is significantly larger and $i_{lim}/\omega^{1/2}$ varies with ω. Thus, it seems advisable to carry out the RRDE experiment in a manner which yields both collection efficiency and limiting ring and disk current data.

Transient behavior.—The simulated ring current transients for the ECE mechanism are identical to those for the EC mechanism. For the first- and second-order catalytic reactions, the value of $\omega t (D/\nu)^{1/3} (0.51)^{2/3}$ at which the ring current is one-half of the steady-state value is observed to be a function of *XKT* or *XKTC* as in the EC case. Unlike the EC transients, however, the catalytic transients do not exhibit maxima.

Results and Discussion

To test the simulation results for a second-order catalytic reaction, the reduction of iron(III) in the presence of hydrogen peroxide was investigated. This reaction, previously investigated at a RDE by Haberland and Landsberg (10), was studied by reduction of ferric ion at the disk and analysis for the ferrous ion at the ring, that is

$$Fe^{+3} + e \rightarrow Fe^{+2} \qquad \text{disk electrode}$$

$$Fe^{+2} + 1/2H_2O_2 \xrightarrow{k_2} Fe^{+3} + OH^-$$

$$Fe^{+2} - e \rightarrow Fe^{+3} \qquad \text{ring electrode}$$

The electrode was a carbon paste RRDE with dimensions $r_1 = 0.237$ cm, $r_2 = 0.268$ cm, and $r_3 = 0.455$ cm. It was calibrated by determining the limiting disk and ring currents in a solution containing $6.4 \times 10^{-3}M$ iron(III) and 2*M* HCl. Typical results are shown in Fig. 6, curves b and c. The experimental collection efficiency, 0.545 ± 0.003, compares quite well to that for the simulation in the absence of perturbing reactions, 0.551. A second determination of the collection efficiency, involving oxidation of $5.7 \times 10^{-4}M$ o-dianisidine in 1*M* H_2SO_4 at the disk electrode yielded a collection efficiency of 0.548 ± 0.003.

The limiting disk currents and corresponding limiting ring currents for the solution which was $6.4 \times 10^{-3}M$ in ferric ion and $0.64 \times 10^{-3}N$ in hydrogen peroxide were found to be identical to those obtained in a solution which contained $6.4 \times 10^{-3}M$ ferric ion and no hydrogen peroxide. This indicated that at this ratio of the concentration of ferric ion to hydrogen peroxide, the rate of the ferrous-hydrogen peroxide reaction was so slow that its effect on the ring and disk currents could not be detected.

When limiting ring and disk currents were obtained for the solution which was $6.4 \times 10^{-3}N$ in both ferric ion and hydrogen peroxide, it was obvious that the reaction was significantly affecting the ring and disk currents. These currents along with the collection efficiencies at various rotation rates are shown in Table I. Also shown in Table I are the values of *XKTC* corresponding to the observed collection efficiencies as obtained from the $m = 1.0$ working curve in Fig. 5. The

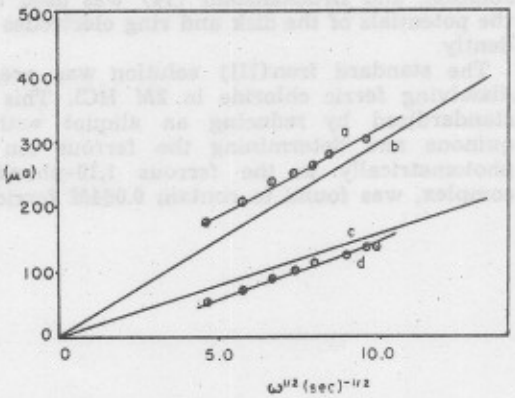

Fig. 6. Experimental limiting ring and disk currents for the ferrous-hydrogen peroxide reaction as compared with simulated values. a. Simulated limiting disk current in the presence of a catalytic following reaction. b. Limiting disk current in the absence of a following reaction. c. Limiting ring current in the absence of a following reaction. d. Simulated limiting ring current in the presence of a catalytic following reaction. ⊙ Experimental results.

Table I. RRDE data for the iron(III)-hydrogen peroxide system[a]

ω (sec^{-1})	Disk current i_d (μA)	Ring current i_r (μA)	N_A[b]	$XKTC$[c]	$(XKTC) \times (\omega)$	k_2 (liter/mole sec)
21.4	177	53	0.300	0.59	12.6	100
32.6	208	73	0.351	0.40	13.1	104
43.9	238	91	0.383	0.30	13.4	105
53.6	250	104	0.416	0.23	12.3	98
62.8	264	114	0.432	0.20	12.6	100
91.4	302	136	0.450	0.16	14.6	116
97.8	297	136	0.458	0.14	13.7	109
					Avg. k_2 =	105 ± 5

[a] The solution was 6.4 x $10^{-3}N$ in both Fe(III) and H_2O_2 and 2M in HCl. The carbon paste RRDE had the dimensions r_1 = 0.237 cm, r_2 = 0.268 cm, r_3 = 0.455 cm. The temperature was 23°C.
[b] $N_A = -i_r/i_d$.
[c] Calculated using simulated curves in Fig. 5.

product of the rotation rate and the value of $XKTC$

$$(\omega)(XKTC) = k_2 C^o_A (\nu/D_A)^{1/3} (0.51)^{-2/3}$$

should also be a constant. The values of this product and also the value of k_2 calculated for each rotation rate using a value of the diffusion coefficient, D_A, of 5 x 10^{-6} cm^2/sec and a value of the kinematic viscosity, ν, of 1 x 10^{-2} cm^2/sec, are also given in Table I.

The average value of k_2, 105 liters/mole-sec, compares favorably with reported values which range from k_2 = 96 liters/mole-sec in a solution containing 2M chloride ion and 4 x $10^{-3}M$ hydrogen ion at 35°C (12), to k_2 = 145 obtained in a 1M potassium chloride solution (10). This average value of k_2, calculated using the collection efficiencies, can also be employed to compare the predicted values of disk and ring current to the experimental ones. Curves a and d in Fig. 6 are the results of simulations of i_d and i_r at different values of ω employing a k_2 of 105 liters/mole-sec and parameters from the experimental ring and disk currents in the absence of hydrogen peroxide. Also shown in Fig. 6 are the experimental values of i_d and i_r from Table I, which are in satisfactory agreement with the simulated values.

Experimental

The carbon paste RRDE was fabricated from a cylinder of Quickmount (E. H. Sargent Company, Chicago, Illinois) molded onto a precision steel shaft (13). A Motormatic E-550 motor and controller (Electrocraft Corporation, Hopkins, Minnesota) was used as a rotator. A 1/4-in. chuck was mounted directly onto the motor shaft and held the RRDE. A dual-potentiostat similar to that described by Napp, Johnson, and Bruckenstein (14) was used to control the potentials of the disk and ring electrodes independently.

The standard iron(III) solution was prepared by dissolving ferric chloride in 2M HCl. This solution, standardized by reducing an aliquot with hydroquinone and determining the ferrous ion spectrophotometrically as the ferrous 1,10-phenanthroline complex, was found to contain 0.064M ferric ion.

A stock solution of hydrogen peroxide was prepared by diluting an approximately 30% hydrogen peroxide solution with water to produce about a 5 x $10^{-3}M$ solution. The hydrogen peroxide concentration of this solution was determined shortly before the experiment by reacting an aliquot of this solution with an aliquot of a standard solution of ferrous ammonium sulfate and determining the amount of ferrous ion remaining in solution spectrophotometrically. The hydrogen peroxide solution was found to be 5.9 x $10^{-3}M$ in hydrogen peroxide, or 1.18 x $10^{-2}N$ as an oxidant in the ferrous-hydrogen peroxide reaction. Test solutions were prepared from these stock solutions.

Solutions more concentrated than 6.4 x $10^{-3}N$ in hydrogen peroxide were found to be unstable with respect to decomposition into oxygen and water. Even in a solution which was 6.4 x $10^{-3}N$ in hydrogen peroxide, bubbles were observed at the electrode surfaces. This required wiping the electrode before each measurement and making the measurement as rapidly as possible. All measurements were carried out at 23° ± 0.5°C.

Acknowledgment

The support of the Mobil Oil Corporation and the Eastman Kodak Company for fellowships to one of us (K.B.P.) the Robert A. Welch Foundation, and the National Science Foundation are gratefully acknowledged.

Manuscript submitted April 7, 1970; revised manuscript received July 22, 1970.

Any discussion of this paper will appear in a Discussion Section to be published in the June 1971 JOURNAL.

REFERENCES

1. K. B. Prater and A. J. Bard, *This Journal*, **117**, 207 (1970).
2. W. J. Albery and S. Bruckenstein, *Trans. Faraday Soc.*, **62**, 1920 (1966).
3. K. B. Prater and A. J. Bard, *This Journal*, **117**, 335 (1970).
4. W. J. Albery and S. Bruckenstein, *Trans. Faraday Soc.*, **62**, 1946 (1966).
5. W. J. Albery and S. Bruckenstein, *ibid.*, p. 2584.
6. W. J. Albery, M. L. Hitchman, and J. Ulstrup, *ibid.*, **64**, 2831 (1968).
7. W. J. Albery, M. L. Hitchman, and J. Ulstrup, *ibid.*, **65**, 1101 (1969).
8. L. S. Marcoux, R. N. Adams, and S. Feldberg, *J. Phys. Chem.*, **73**, 2611 (1969).
9. J. Koutecky and V. G. Levich, *Zhur. Fiz. Khim.*, **32**, 1565 (1958).
10. D. Haberland and R. Landsberg, *Z. Elektrochem.*, **70**, 724 (1966).
11. P. Beran and S. Bruckenstein, *J. Phys. Chem.*, **72**, 3630 (1968).
12. C. F. Wells and M. A. Salam, *Trans. Faraday Soc.*, **63**, 620 (1967).
13. P. A. Malachesky, K. B. Prater, G. Petrie, and R. N. Adams, *J. Electroanal. Chem.*, **16**, 41 (1968).
14. D. T. Napp, D. C. Johnson, and S. Bruckenstein, *Anal. Chem.*, **39**, 481 (1967).

Reprinted from JOURNAL OF THE ELECTROCHEMICAL SOCIETY
Vol. 117, No. 12, December 1970
Printed in U.S.A.